applied sciences

MDPI

Article

In Silico Identification of Six Mushroom-Derived Sterol and Triterpenoid Compounds as Potential P-Glycoprotein Modulators in Multidrug Resistance

Jéssica Fonseca [1,2,3], Carlos S. H. Shiraishi [4,5], Rui M. V. Abreu [4], Sara Ricardo [1,2,6,*,†] and Josiana A. Vaz [3,4,*,†]

1 UCIBIO—Applied Molecular Biosciences Unit, Toxicologic Pathology Research Laboratory, University Institute of Health Sciences (UCIBIO-IUCS-CESPU), 4585-116 Gandra, Portugal; jessica.fonseca@ipb.pt
2 Associate Laboratory i4HB—Institute for Health and Bioeconomy, University Institute of Health Sciences—CESPU, 4585-116 Gandra, Portugal
3 Research Centre for Active Living and Wellbeing (LiveWell), Instituto Politécnico de Bragança, 4585-116 Bragança, Portugal
4 CIMO, SusTEC, Instituto Politécnico de Bragança, Campus de Santa Apolónia, 5300-253 Bragança, Portugal; shiraishi@ipb.pt (C.S.H.S.); ruiabreu@ipb.pt (R.M.V.A.)
5 Nutrition and Bromatology Group, Department of Analytical Chemistry and Food Science, Instituto de Agroecoloxía e Alimentación (IAA)—CITEXVI, Universidade de Vigo, 36310 Vigo, Spain
6 Differentiation and Cancer Group, Institute for Research and Innovation in Health (i3S), University of Porto, 4099-002 Porto, Portugal
* Correspondence: sara.ricardo@iucs.cespu.pt (S.R.); josiana@ipb.pt (J.A.V.)
† These authors contributed equally to this work.

Abstract

The overexpression of P-glycoprotein (P-gp) is often directly related to multidrug resistance (MDR), one of the greatest challenges in cancer treatment. This transmembrane efflux pump decreases the intracellular concentrations of chemotherapy drugs, reducing their effectiveness and resulting in treatment failure. This work used in silico methods to assess the potential of bioactive chemicals produced from mushrooms as P-gp modulators. A database comprising 211 bioactive compounds from mushrooms was investigated using molecular docking and virtual screening techniques against the P-gp structure. The compounds ergosta-4,6,8(14),22-tetraen-3-one, lucidumol A, (22*E*,24*S*)-ergosta-4,22-dien-3-one, antcin K, 3,11-dioxolanosta-8,24(*Z*)-diene-26-oic acid, and (22*E*)-19-norergosta-5,7,9,22-tetraen-3β-ol were identified as the six best candidates from our database of mushroom compounds based on their binding affinities, toxicity predictions, and pharmacological properties assessed through ADME analyses (absorption, distributions, metabolism, and excretion). These six compounds exhibited strong binding affinities, with binding energies ranging from −12.31 kcal/mol to −10.93 kcal/mol, all showing higher affinities than the control, tariquidar, which had a binding energy of −10.78 kcal/mol. Toxicity predictions indicated favorable safety profiles for all six, while ADME analyses found that all six compounds had high oral bioavailability and a low probability of acting as P-gp substrates. These results position bioactive mushroom compounds, particularly these six, as promising P-gp modulators, suggesting positive outcomes in cancer treatment.

Keywords: mushrooms; P-glycoprotein; virtual screening; multidrug resistance

Academic Editor: Fabrizio Carta

Received: 11 July 2025
Revised: 1 August 2025
Accepted: 2 August 2025
Published: 8 August 2025

Citation: Fonseca, J.; Shiraishi, C.S.H.; Abreu, R.M.V.; Ricardo, S.; Vaz, J.A. In Silico Identification of Six Mushroom-Derived Sterol and Triterpenoid Compounds as Potential P-Glycoprotein Modulators in Multidrug Resistance. *Appl. Sci.* **2025**, *15*, 8772. https://doi.org/10.3390/app15168772

1. Introduction

One of the main obstacles to the successful treatment of cancer is the control of multidrug resistance (MDR). A protein expressed by the MDR1 gene, also called

P-glycoprotein (P-gp) or ABCB1, which is a member of the B superfamily of ATP-binding cassette transporter (ABCs), is one of the main causes of this phenomenon [1,2]. This energy-dependent efflux pump, located in the plasma membrane, is responsible for transporting substrates across the cell membrane [3,4]. Numerous tumor cell types have already been found to have overexpressed P-gp, which acts by increasing the efflux of chemotherapeutic drugs and reduces intracellular accumulation, thus decreasing the drug's efficacy [5]. Consequently, the failure of some chemotherapy treatments, including doxorubicin, paclitaxel, and topotecan, which are mediated by this efflux mechanism, is directly linked to the increased expression of P-gp [6]. P-gp is a polypeptide with 1280 residues and a mass of 170 kDa. P-gp's structure consists of two nucleotide-binding domains (NBDs) and two transmembrane domains (TMDs) (Figure 1) [3]. While the TMDs are composed of six hydrophobic α-helices that allow the drug to cross the membrane through internal and external conformations, the NBDs are necessary for the binding and hydrolysis of ATP, which provides energy for the conformational change needed to transport the drug out of the cells [7]. The operational process of P-gp includes switching between inward- and outward-facing forms, in which ATP binds to the NBDs to initiate a conformational change that allows the bound substrate's release [3]. Given the importance of P-gp in MDR, different methods have been investigated to increase the effectiveness of drug administration. There are three ways to prevent P-gp activity: compounds blocking the binding sites, interrupting ATP degradation, and altering the lipid structure of the cell membrane [6]. There are currently three generations of P-gp inhibitors, but all of them have some level of toxicity. The first generation (e.g., verapamil and cyclosporine A) showed low MDR reversal activity and high toxicity; the second generation (e.g., biricodar) showed greater efficacy but unpredictable drug interactions, limiting its use; and the third generation (tariquidar) showed high specificity but also failed in clinical trials due to toxicity [7,8]. Despite the efforts and advances made in developing P-gp inhibitors over the last few decades, the first three groups of inhibitors failed in the clinical testing phase, mainly due to the toxicity associated with the doses needed to block the action of P-gp [7]. Figure 2 shows the groups of inhibitors developed and their respective mechanisms of action and generations. Acknowledging these compounds' limitations, searching for natural P-gp inhibitors has emerged as a promising strategy. Approximately 70% of current anticancer drugs are derived from natural products [9]. Natural compounds, such as those from plants and fungi, are considered less harmful in reversing tumor resistance due to their relatively low toxicity to normal cells [2]. Thanks to this, and to the bioactive potential of their secondary metabolites, mushrooms have been used for many years in traditional Chinese medicine and have, therefore, often been considered a natural choice for cancer treatment [10]. Numerous investigations have demonstrated that the bioactive substances found in mushrooms can inhibit MDR [9,11–14]. Other studies have reported that these compounds could act as effective modulators of P-gp, improving drug retention in resistant cancer cells [15–18]. A recent systematic review published by our research group discussed the potential of mushroom extracts in regulating P-gp expression [19]. Molecular docking is widely used to predict the interactions between ligands and proteins, allowing potential therapeutic targets to be analyzed [20]. Using this computational technique, this study aimed to utilize a database of 211 bioactive mushroom compounds, which was part of a database developed at the Polytechnic Institute of Bragança, located in the Trás-os-Montes region of Portugal. This database was initially created in [21] and later updated and extended in [22,23].

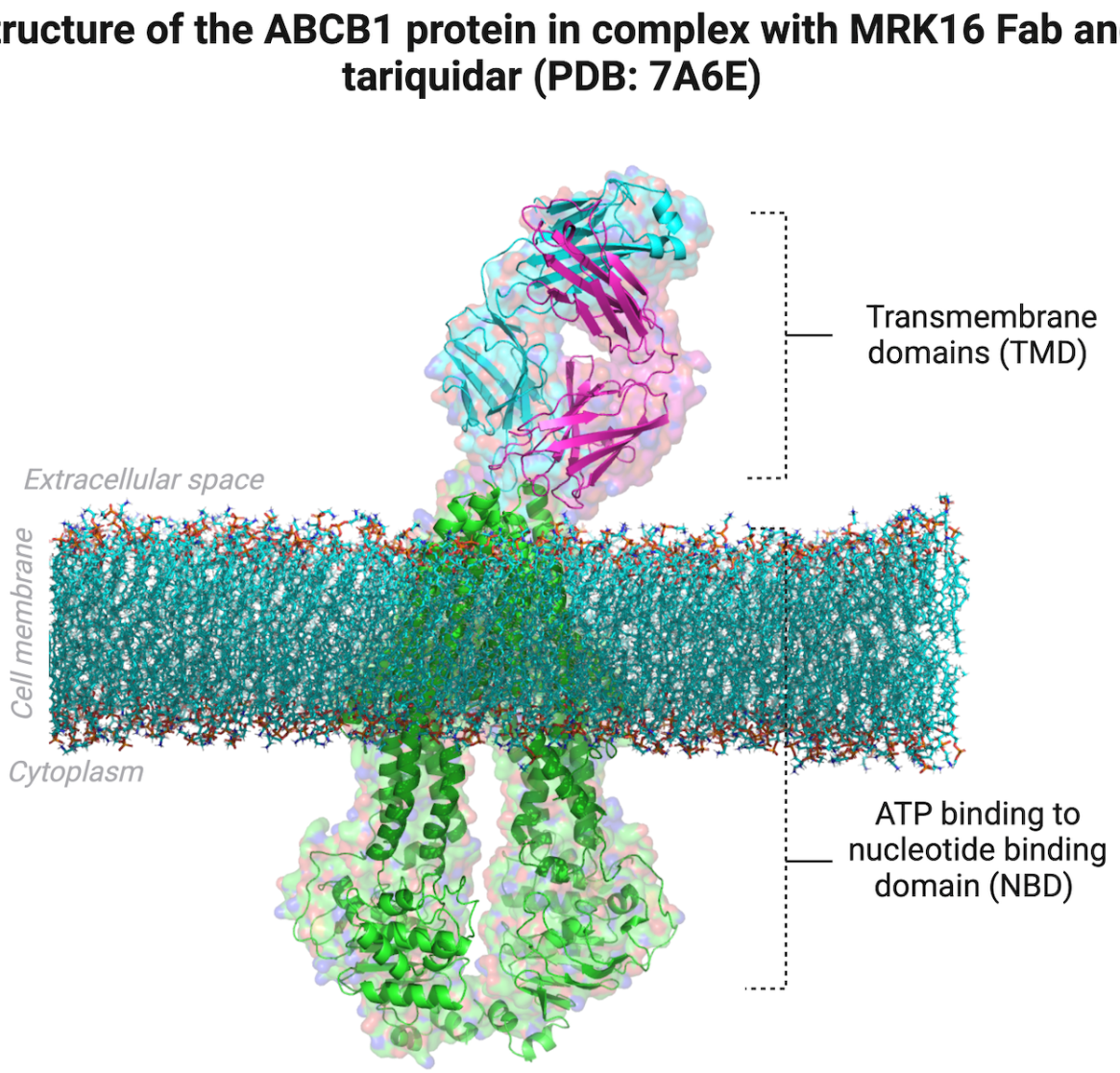

Figure 1. The ABCB1 protein (P-glycoprotein) structure in complex with the Fab antibody MRK16 and the inhibitor tariquidar (PDB: 7A6E).

The relevance of bioactive compounds derived from mushrooms is especially noteworthy in cancer research, given their therapeutic potential, as demonstrated in various studies. These compounds, which include polysaccharides, terpenoids, and phenolic derivatives, have shown the ability to induce apoptosis, modulate the immune response, and inhibit tumor progression. Thus, this database constitutes a valuable tool for the development of new treatment strategies and the advancement of cancer research. With the aim of identifying promising modulators of P-pg protein activity, this study proposes an in silico evaluation of the possible interactions between the compounds in this database and the protein in a virtual environment. In addition, the toxicity predictions, pharmacokinetic characteristics, and safety profiles of the compounds from the database were evaluated in ADME studies. Through this approach, we identified six compounds with high predicted efficacy against P-pg and low predicted toxicity, which could be promising candidates for future in vitro studies.

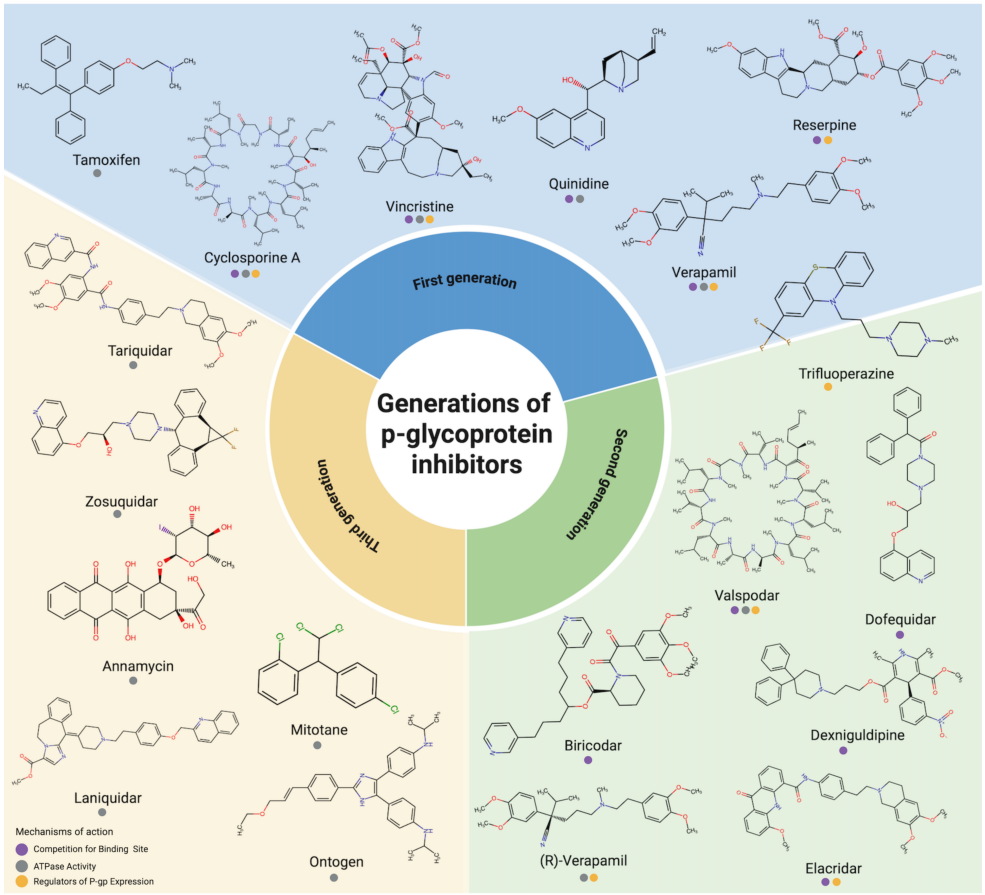

Figure 2. Generations of P-glycoprotein inhibitors and their respective mechanisms of action. The table categorizes the compounds by generation and lists their respective mechanisms of action, including competition for binding sites, the modulation of ATPase activity (stimulating or inhibiting), and the regulation of P-gp expression (up or down). References for each compound: Verapamil [11,12], Ciclosporin A [12,13], Vincristine [12], Reserpine [12], Quinidine [12], Tamoxifen [12], (R)-Verapamil [12], Dexniguldipine [12], Elacridar [12,14], Biricodar [12], Dofequidar [12], Trifluoperazine [12], Valspodar [12], Tariquidar [12,24], Zosuquidar [14,24], Laniquidar [24,25], Ontogen [14,24], Mitotane [24,26], and Anamycin [24,27].

2. Materials and Methods

2.1. Molecular Docking

2.1.1. Database of Bioactive Mushroom Compounds

This study used the mushroom compound database initially created by CFR Ferreira et al. (2010) [21] and later updated and extended by Borges (2018) [22] and Shiraishi (2020) [23] (https://cshiraishi.github.io/LMW-Database/) (accessed on 29 January 2025). The database includes 211 mushroom-derived compounds, which were the focus of this work. The 3D structures of the compounds were generated using the DataWarrior software (Version 06.04.02) [28] and then exported to the YASARA software [29] (Version 24.4.10), where the structures of the 211 compounds were prepared for subsequent molecular docking.

2.1.2. Protein Structure Preparation

The structure of P-glycoprotein (PDB: 7A6E) [30] was obtained from the Protein Data Bank. This structure was experimentally obtained by cryoelectron microscopy, with a resolution of 3.60 Angstroms (Å). It was chosen as it is from *Homo sapiens* and is coupled to tariquidar, a third-generation P-gp inhibitor. To prepare the structure of P-gp, we followed a careful workflow. Initially, the 7A6E.pdb file was edited using the YASARA software

to remove binding molecules (such as the inhibitor tariquidar, cholesterol molecules, and water) and unnecessary records (such as TER and CONNECT), resulting in a clean protein. Next, we used a common text editor to review this process, ensuring the complete removal of non-essential elements. After this step, the edited structure was subjected to energy minimization using the YAMBER3 force field in YASARA, ensuring the stable and adequate conformation of the protein for subsequent docking studies. Following these preparation steps, a three-dimensional grid box was created in the region corresponding to the protein's active site based on the original location of the tariquidar inhibitor in the experimental structure. The X, Y, and Z grid dimensions were 30 Å × 30 Å × 30 Å, and the selected center of the grid box was positioned at coordinates X = 164, Y = 155, Z = 154 of the PDB structure used (PDB: 7A6E). In addition, a membrane environment was built using the YASARA script md_runmembrane.mcr, allowing a more accurate simulation of the protein's behavior in its native lipid bilayer context. The grid preparation steps were performed using the YASARA software, and the scripts used are also available in YASARA [29]. In the membrane model, we used phosphatidylethanolamine (PEA), a common lipid known for its stability. The Z coordinates of the atoms indicated a mean plane around $Z \approx 0$. PEA molecules were evenly distributed across both leaflets, with 49.7% in the upper leaflet and 50.3% in the lower leaflet. All lipids were assumed to be 1-palmitoyl-2-oleoyl by default. It was recommended that the simulation be carried out at physiological pH (pH = 7.4). A 0.9% NaCl solution, which is representative of a normal physiological configuration, was used to define the ion concentration. A temperature of 298 K was used for the simulation.

2.1.3. Redocking and Validation

Redocking studies were performed using the AutoDock VINA algorithm [31] integrated into the YASARA software [29]. We used the prepared 7A6E protein to validate the active site. Tariquidar was rocked using blind site docking to confirm its interaction with the expected binding site. The best poses were selected and compared with the tariquidar co-crystallized in the original protein structure. The root mean square deviation (RMSD) was calculated using the DockRMSD software [32] (https://zhanggroup.org/DockRMSD/) (accessed on 5 February 2025). Based explicitly on all heavy atoms of the best docking poses and the co-crystallized tariquidar conformation. The resulting RMSD value of 1.60 Å corresponded to the structural deviation between these two conformations. Since this value was below the commonly accepted threshold of 2 Å, it indicated that the docking method was reliable.

2.1.4. Virtual Screening

Virtual screening was also carried out using the AutoDock VINA algorithm [31]. The database of 211 mushroom-derived bioactive compounds, represented in their 3D structures, was processed with the previously prepared protein using the script YASARA Dock_runscreening.mcr, an automated tool designed for large-scale docking screenings. After running the script, the results of the simulations were visualized with the PyMOL Molecular Graphics System, Version 3.0.5, Schrödinger, LLC [33], and the molecular interactions were analyzed with the Protein Plus software [34] (https://proteins.plus) (accessed on 10 February 2025). Initially, to define the active site, a three-dimensional grid box was generated with grid dimensions of 30 Å, 30 Å, and 30 Å, adequately covering the region of interest in the protein. The center of the box was positioned at coordinates X = 164, Y = 155, Z = 154 of the PDB structure used (PDB: 7A6E), corresponding to the location of the tariquidar inhibitor in the co-crystallized structure. All simulations were performed using standard personal computer hardware, sufficient for molecular docking and virtual screening tasks.

2.2. Toxicity Prediction

The best-predicted toxic effect of the screened mushroom-derived database of bioactive compounds was analyzed using the ProTox 3.0 software [35]. This software evaluates the compounds' toxicity by calculating several parameters, including organ toxicity, such as hepatotoxicity, neurotoxicity, nephrotoxicity, respiratory toxicity, and cardiotoxicity. In addition, ProTox 3.0 calculates toxicity endpoints such as carcinogenicity, immunotoxicity, mutagenicity, cytotoxicity, blood–brain barrier (BBB) toxicity, ecotoxicity, clinical toxicity, and nutritional toxicity. Regarding nuclear receptor signaling pathways, the effects of each compound in different relevant proteins were also calculated, including the aryl hydrocarbon receptor (AhR), androgen receptor (AR), ligand-binding domain (AR-LBD), aromatase estrogen receptor alpha (ER), estrogen receptor ligand-binding domain (ER-LBD), and peroxisome proliferator-activated receptor gamma (PPAR-Gamma). Cellular stress response pathways were also investigated, including nuclear factor (erythroid-derived 2)-like 2/antioxidant responsive element (nrf2/ARE), heat shock factor response element (HSE), mitochondrial membrane potential (MMP), phosphoprotein (tumor suppressor) p53, and ATPase family AAA domain-containing protein 5 (ATAD5). The analysis of molecular initiating events included thyroid hormone receptor alpha (THRα), thyroid hormone receptor beta (THRβ), transtyretrin (TTR), ryanodine receptor (RYR), GABA receptor (GABAR), glutamate N-methyl-D-aspartate receptor (NMDAR), alpha-amino-3-hydroxy-5-methyl-4-isoxazolepropionate receptor (AMPAR), kainate receptor (KAR), acetylcholinesterase (AChE), constitutive androstane receptor (CAR), pregnane X receptor (PXR), NADH-quinone oxidoreductase (NADHOX), the voltage-gated sodium channel (VGSC), and Na+/I− symporter (NIS). Finally, the effect on the metabolism of the compounds was analyzed, considering the cytochromes CYP1A2, CYP2C19, CYP2C9, CYP2D6, CYP3A4, and CYP2E1. A qualitative score was created to classify the compounds, in which the 'inactive' state received 1 point, indicating that the compound did not present toxicity in the evaluated parameter, while the 'active' state received 0 points, indicating toxicity. Thus, the higher the score, the less toxic the compound was, considering a qualitative evaluation of the analyzed parameters. In this way, at the end of the evaluation, the compounds with the highest scores exhibited less toxicity, helping to select those with the most significant potential.

2.3. ADME Analysis

The bioactive compounds' absorption, distribution, metabolism, and excretion (ADME) predictions were carried out using the SwissADME software [36] (http://www.swissadme.ch) (accessed on 5 March 2025). During this analysis, crucial parameters were assessed, such as whether the compound was a P-gp substrate, gastrointestinal (GI) absorption (GI), blood–brain barrier (BBB) permeability, and compliance with Lipinski's Rule of Five. Based on these parameters, a scoring system was created to classify the compounds more objectively and qualitatively. In the case of P-gp, compounds that were not substrates scored 2 points, while compounds that were substrates scored 0 points. Regarding GI absorption, compounds with high absorption scored 1 point, while those with low absorption scored 0 points. For BBB permeability, compounds that did not exceed the BBB scored 1 point, while those that did exceed it scored 0. As for Lipinski's Rule of Five, if there was no violation of the conditions, the compounds received 2 points. If the software signaled that a compound exhibited only one violation, the compound scored 1 point. If the software gave a negative signal or there were one or more significant violations, the compound scored 0 points. In this way, the compounds with the highest potency showed the greatest potential for efficacy and safety.

3. Results

3.1. Molecular Docking

3.1.1. Protein Structure and Redocking Validation

In this study, we adopted a layered approach where, at each stage, we selected the most promising compounds, as diagrammed in Figure 3.

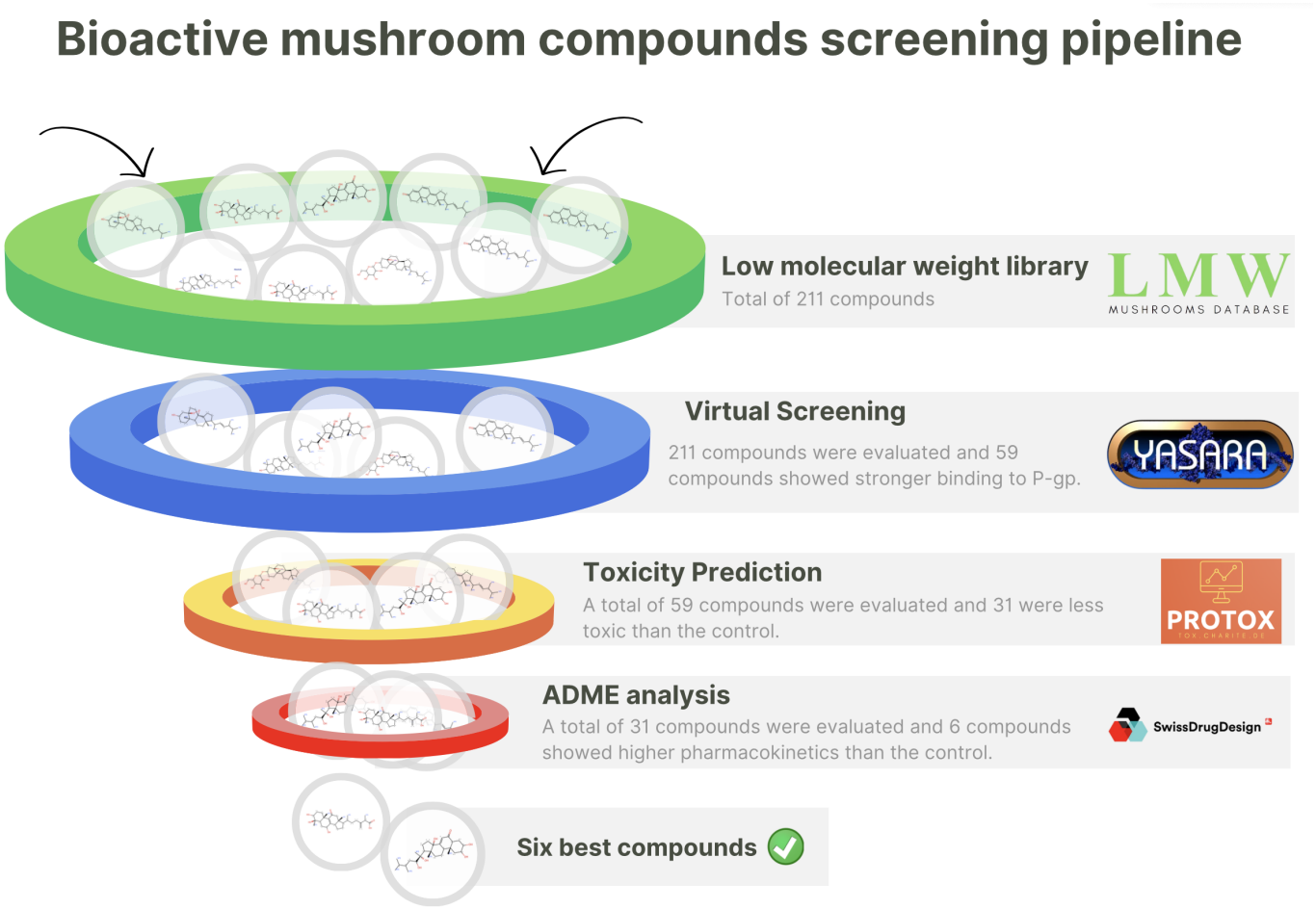

Figure 3. Bioactive mushroom compound screening pipeline.

The redocking analysis was carried out using the AutoDock VINA software [31], and compounds were classified based on the binding energy (kcal/mol), which ranged from −11.31 to −10.39 kcal/mol (Table S1, Supplementary Materials). After redocking the isolated tariquidar with the 7A6E protein [30], we compared the pose obtained with the poses (Table S2, Supplementary Materials) of the tariquidar co-crystallized in the original protein structure, as shown in Figure 4A). The RMSD obtained was 1.60 Å. The main interaction area included residues widely distributed in different protein domains, as shown in Figure 4B), highlighting their relevance in molecular interactions. The results validate the methodology and establish a solid basis for subsequent analyses of the interactions between mushroom-derived bioactive compounds and the P-gp protein.

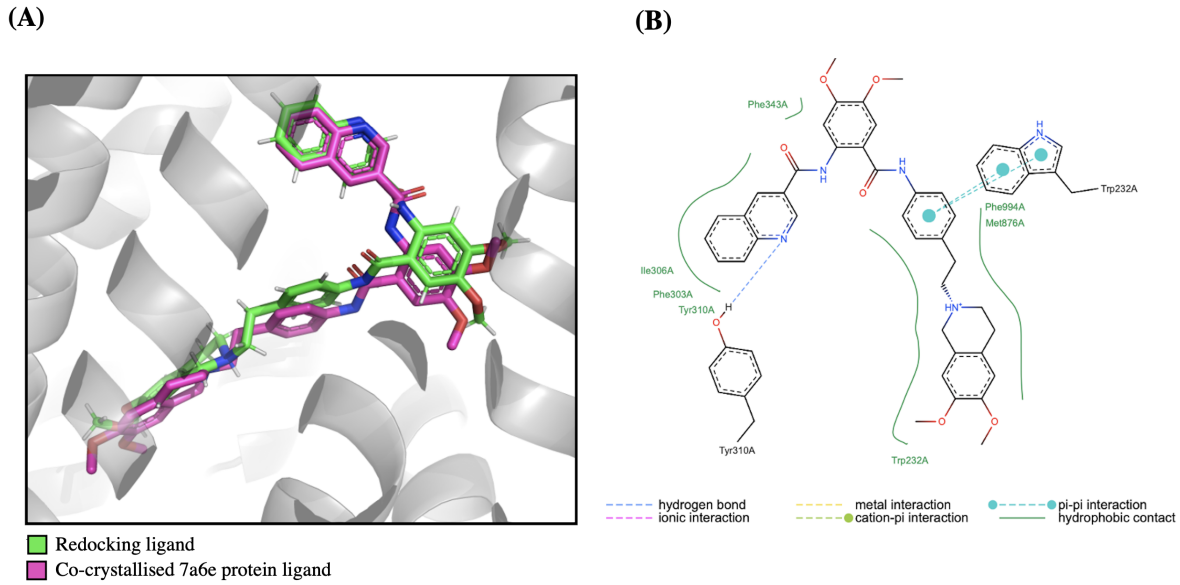

Figure 4. Redocking of the isolated tariquidar with the P-gp protein (PDB: 7A6E). (**A**) shows the redocking ligand in green and the co-crystallized ligand of the 7A6E protein in pink. (**B**) illustrates the interaction area, highlighting residues distributed across different protein domains and their contributions to molecular interactions.

3.1.2. Virtual Screening

An in silico analysis investigated the interaction between the database of bioactive mushroom compounds and the P-pg (PDB: 7A6E) structure. The initial objective was to perform a virtual screening to identify the compounds with the best-predicted affinity for P-gp, highlighting the most promising P-gp inhibitor candidates. The mushroom compound database, as detailed in Section 2, was used for screening [21–23]. The predicted binding energy values, calculated using the AutoDock VINA docking software, were used as a selection criterion, with lower values indicating greater predicted affinity between the compounds and the P-pg protein.

The binding energies of the bioactive compounds ranged from −13.19 to 0.07 kcal/ mol (Table S3, Supplementary Materials). With a binding energy of −10.78 kcal/ mol, the well-known and potent P-gp inhibitor tariquidar was used as a positive control and screening reference. The compounds with the highest binding energies compared to the positive control were (22*E*,24*S*)-ergosta-4,22-dien-3-one (−12.31 kcal/mol), lanostanoid 4 (−13.19 kcal/mol), and lanostanoid 3 (−12.67 kcal/mol). Analyzing the complete database of 211 compounds, 59 showed lower (more negative) predicted binding energies than the tariquidar used as a control, indicating a better predicted binding affinity to the P-gp protein (Table 1). Other compounds, such as ergosterols, also showed higher affinity, with ergosterol showing a predicted binding energy of −12.31 Kcal/mol, well below the value obtained for tariquidar of −10.78 kcal/mol. Regarding the molecular contact surface (Con.Surf[A^2]), the control tariquidar stood out with a larger area (633.75 A^2) compared to the other compounds from the database. This value is due to its large and bulk structure (Figure 5). From the mushroom database, some compounds, such as officimalonic acids C (554.09 A^2) and officimalonic acids E (550.17 A^2), also presented large areas, albeit still lower than that of tariquidar. On the other hand, molecules such as ergosta-4,6,8(14),22-tetraen-3-one (367.21 A^2) and (22*E*)-19-norergosta-5,7,9,22-tetraen-3β-ol (384.84 A^2) exhibited more compact surfaces.

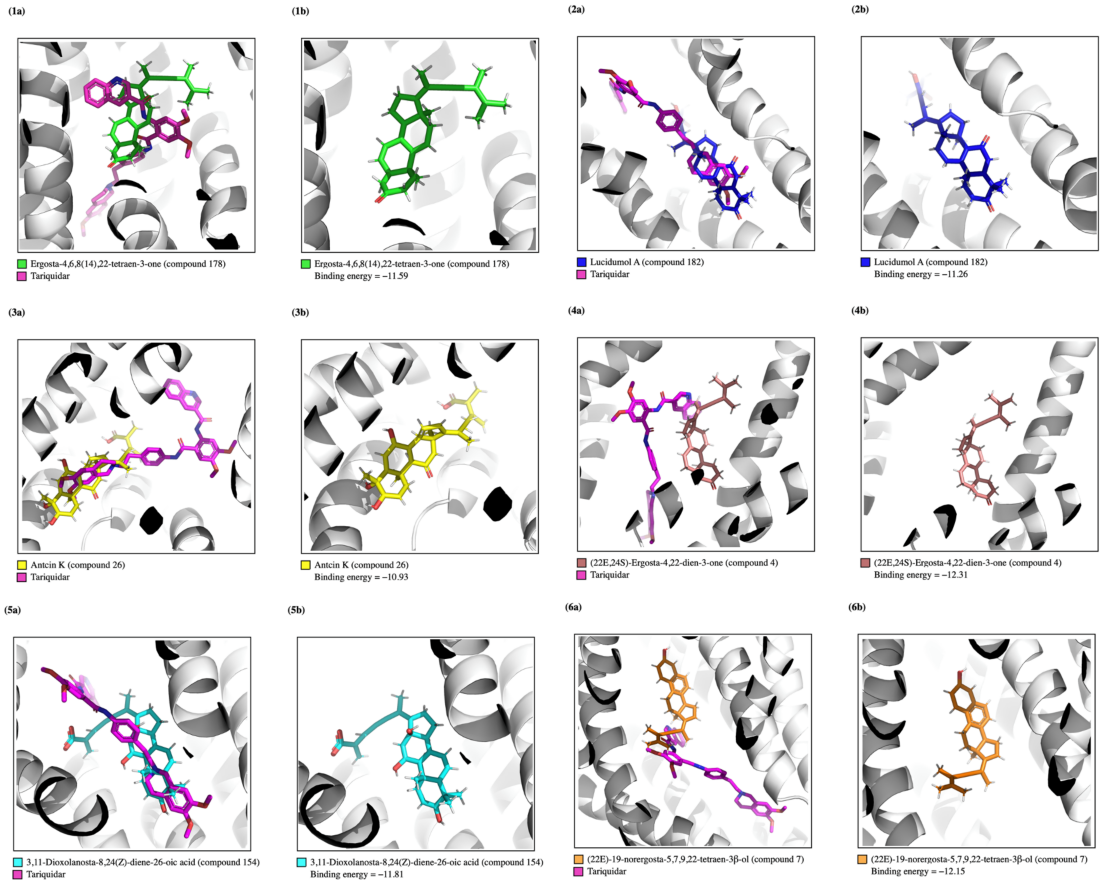

Figure 5. Best mushroom-derived bioactive compounds interacting with the P-gp protein (PDB: 7A6E), evaluated in comparison with the tariquidar control. (**1a**,**2a**,**3a**,**4a**,**5a**,**6a**) illustrate the compounds compared to the control, while (**1b**,**2b**,**3b**,**4b**,**5b**,**6b**) show only the isolated compounds. Ergosta-4,6,8(14),22-tetraen-3-one ((**1a**) compared to control and (**1b**) isolated compound), lucidumol A ((**2a**) compared to control and (**2b**) isolated compound), antcin K ((**3a**) compared to control and (**3b**) isolated compound), (22*E*,24*S*)-ergosta-4,22-dien-3-one ((**4a**) compared to control and (**4b**) isolated compound), 3,11-dioxolanosta-8,24(*Z*)-diene-26-oic acid ((**5a**) compared to control and (**5b**) isolated compound), and (22*E*)-19-norergosta-5,7,9,22-tetraen-3β-ol ((**6a**) compared to control and (**6b**) isolated compound).

Table 1. Compounds with better binding energies.

Compound	Name	Predicted Binding Energy [kcal/mol]	Con.Surf [Å^2]
121	Lanostanoid 4	−13.19	470.73
120	Lanostanoid 3	−12.67	495.39
4	(22*E*,24*S*)-Ergosta-4,22-dien-3-one	−12.31	461.12
177	Ergosterol	−12.27	462.35
68	Inoscavin A	−12.22	445.33
7	(22*E*)-19-Norergosta-5,7,9,22-tetraen-3β-ol	−12.15	384.84
111	Officimalonic acids D	−12.09	565.94
1	+E4:F38(3β,5α,8α,22*E*,24*S*)-5,8-Epidioxyergosta-6,9(11),22-trien-3-ol	−12.07	448.19
21	9,11-Dehydroergosterol peroxide	−12.04	449.10
10	(22*E*)-Ergosta-5,7,22-trien-3β-ol	−12.01	457.70
9	(22*E*)-5α,6α-Epoxyergosta-8,14,22-triene-3β,7β-diol	−11.98	447.32
3	3β,5α,8α,22*E*)-5,8-Epidioxyergosta-6,22-dien-3-ylβ-D-glucopyranoside	−11.93	506.27

Table 1. *Cont.*

Compound	Name	Predicted Binding Energy [kcal/mol]	Con.Surf [Å^2]
12	(3β,5α,22*E*)-Ergosta-7,22,24(28)-trien-3-ol	−11.92	455.67
23	Eburicoic acid	−11.91	467.92
32	Ergosterol peroxide	−11.87	465.10
168	3-Oxo-24-methyl-5α-lanost-8,25-dien-21-oic acid	−11.86	476.27
171	22E-5α-Ergost-7,9(11),22-trien-3β-ol	−11.84	466.39
154	3,11-Dioxolanosta-8,24(*Z*)-diene-26-oic acid	−11.81	444.14
194	Ganoderic Acid T	−11.74	587.44
124	Acetyl-3-oxo-sulfurenic acid (64)	−11.74	512.85
17	5α,6α-Epoxy-24(*R*)-methylcholesta-7,22-dien-3β-ol	−11.73	437.11
190	Ganoderic Acid H	−11.66	503.58
112	Officimalonic acids E	−11.66	550.17
48	Colossolactone H (Colo H)	−11.64	469.63
178	Ergosta-4,6,8(14),22-tetraen-3-one	−11.59	367.21
114	Officimalonic acids G	−11.52	562.15
193	Ganoderic Acid Y	−11.49	459.87
20	5α,6α-Epoxyergosta-8(14)-ene-3β,7α-diol	−11.48	455.29
139	Inonotsuoxides A	−11.48	438.71
181	Cerevisterol	−11.46	441.80
13	24-Ethylcholesta-5,22-dien-3β-ol	−11.33	390.82
28	Estelasterol	−11.31	408.88
191	Ganoderic Acid W	−11.30	533.11
19	5α,8α-Epidioxy-24(*R*)-methylcholesta-6,22-dien-β-ol	−11.29	426.07
195	Polyporenic acid C	−11.28	472.30
182	Lucidumol A	−11.26	507.86
144	Chagabusone A	−11.23	466.75
34	Polyporusterone A	−11.22	466.28
45	Aurisin A	−11.18	429.27
126	Inonotusol B	−11.14	443.88
6	(22E)-6β-Methoxyergosta-7,22-diene-3β,5α-diol	−11.11	463.33
132	Spiroinonotsuoxodiol	−11.06	469.46
192	Ganoderic Acid X	−11.04	492.63
27	Eringiacetal A	−11.00	388.48
189	Ganoderic acid F	−11.00	481.37
110	Officimalonic acids C	−10.99	554.09
118	Lanostanoid 1 (58)	−10.95	472.98
133	Inonotsudiol A	−10.95	455.79
26	Antcin K	−10.93	496.48
140	Inonotsuoxides B	−10.92	426.16
102	Piptolinic acid E	−10.92	487.53
8	(22E)-3β,5α,9α-Trihydroxyergosta-7,22-dien-6-one	−10.91	410.35
18	5α,8α-Epidioxy-24(*R*)-methylcholesta-6,22-dien-3β-D-glucopyranoside	−10.88	554.78
130	Inonotusol F	−10.87	451.37
113	Officimalonic acids F	−10.87	549.20
11	(22*E*)-Ergosta-7,22-dien-3β-ol	−10.86	425.94
119	Lanostanoid 2	−10.85	502.87
134	Inonotsuoxodiol A	−10.79	478.10
22	Dehydroeburicoic acid	−10.79	480.87
Control	Tariquidar	−10.78	633.80

Only the compounds with the best classification are shown in this table. Complete table available in Supplementary Materials.

3.2. Toxicity Prediction

The compounds evaluated were classified into different toxicity categories based on the predicted LD_{50} values (lethal doses for 50 percent of individuals), and the scale included six classes (Table 2). The compounds defined as class 6, which contains six compounds, have a predicted LD_{50} of more than 10,000 mg/kg, which indicates low toxicity. Class 5 includes 18 compounds with an LD_{50} between 5000 and 10,000 mg/kg, considered potentially dangerous at higher concentrations. Class 4 has 21 compounds with

a predicted LD_{50} between 500 and 5000 mg/kg, which are considered possibly harmful. Nine substances in class 3 are considered dangerous and have a predicted LD_{50} value between 50 mg/kg and 500 mg/kg. Class 2 includes six compounds with a predicted LD_{50} below 50 mg/kg, which are considered highly toxic and can be fatal if ingested. Notably, in this screening, we did not identify any compound with $LD_{50} \leq 5$ mg/kg, which is considered to indicate lethality at such low doses. The organ-specific toxicity analysis revealed that most compounds exhibited a low probability of causing liver damage, and all compounds were classified as inactive for hepatotoxicity (Table S4, Supplementary Materials). However, some compounds showed activity in other organs, such as ergosterol and (22*E*)-ergosta-5,7,22-trien-3β-ol, both associated with neurotoxicity. For nephrotoxicity, officimalonic acid C was identified as toxic. For respiratory toxicity, most of the compounds were predicted to be toxic, suggesting a significant impact on the respiratory system. At the same time, cardiotoxicity was less prevalent, with polyporusterone A presenting a low risk. The control tariquidar, with predicted active toxicity in terms of both nephrotoxicity and respiratory toxicity, and ergosterol, with active predicted toxicity in multiple systems, deserve to be highlighted due to their combined toxicity profile. The analysis of the predicted toxicity endpoints indicated that several bioactive compounds may present carcinogenic potential (Table S4, Supplementary Materials). Although most compounds showed low predicted immunotoxicity, some indicated immunotoxicity, such as polyporenic acid C. These results suggest that certain compounds may impact the immune system. The analyses revealed that most of the compounds evaluated did not show significant mutagenicity, which is beneficial for their development as therapeutic agents. Most compounds showed low predicted cytotoxicity, except for piptolinic acid E, which showed more significant cytotoxic activity. These results indicate that, although some compounds may present toxicity at specific endpoints, many have acceptable toxicological profiles, reinforcing their potential. An analysis of the predicted activity of the mushroom-derived database of compounds against nuclear receptors revealed significant potential in various signaling pathways related to hormonal, metabolic, and inflammatory processes. Compounds such as ganoderic acid (T, W, and X), officimalinic acid, and other lanostanoid derivatives demonstrated active toxicity towards androgen receptors (ARs) and the androgen receptor ligand-binding Domain (AR-LBD). In contrast, compounds such as (22*E*)-19-norergosta-5,7,9,22-tetraen-3β-ol, inonotsudiol A, inonotsuoxodiol A, eburicoic acid, ganoderic acid Y, and others were predicted to be inactive regarding the receptors evaluated. Analyzing the predicted activity in cellular stress response pathways revealed that, although most of the compounds tested did not show activity, some did show toxicity in specific pathways, such as Nrf2/ARE, HSE, and MMP. As an example, inonotusol B and polyporenic acid C showed predicted toxicity in multiple pathways. Notably, none of the compounds tested were predicted to be toxic to p53, which is essential when considering anticancer therapies. Analyses of molecular initiating events revealed that several bioactive compounds, such as ganoderic acid T and ganoderic acid W, showed predicted activity against GABA receptors and pregnane X receptor (PXR). Meanwhile, other compounds, such as 5α,8α-epidioxy-24(R)-methylcholesta-6,22-dien-3β-D-glucopyranoside, polyporusterone A, lucidumol A, and antcin K, proved to be inactive regarding various receptors. Most of the compounds evaluated were predicted to be inactive against CYP1A2, CYP2C19, CYP2C9, CYP2D6, CYP3A4, and CYP2E1, enzymes belonging to the cytochrome P450 (CYP) family, which are essential for the metabolism of medications and other chemical substances in the body [37]. However, some compounds showed specific toxicity in certain isoforms. For example, ergosta-4,6,8(14),22-tetraen-3-one was predicted to be toxic to CYP2C9. Other compounds, such as inonotsol F and the control tariquidar, showed active toxicity to CYP3A4. It is worth noting that many compounds showed

no significant metabolic toxicity in the isoenzymes analyzed, indicating a possible low interaction profile. Based on the methodology described, where 'inactive' compounds scored 1 and 'active' compounds scored 0, the final score offers a qualitative parameter to assess the potential for toxicity, where higher-scoring compounds are considered less toxic and more promising for therapeutic use. The compounds ergosta-4,6,8(14),22-tetraen-3-one and 5α,8α-epidioxy-24(R)-methylcholesta-6,22-dien-3β-D-glucopyranoside, with scores of 309, stand out, with the highest scores, suggesting that they have lower potential for toxicity (Table 2). The complete analysis with all scores for each compound is shown in Table S4 of the Supplementary Materials. On the other hand, compounds with lower scores, such as 3-Oxo-24-methyl-5α-lanost-8,25-dien-21-oic acid (score 124) and officimalonic acids C (score 125), show greater potential for adverse effects and are predicted to be more toxic. Tariquidar, used as a control, obtained a score of 217, a relatively low value. From this comparison, 31 compounds presented a higher score than tariquidar and were predicted to be less toxic and, therefore, were selected for the next screening phase. The final score thus helps to prioritize compounds with the lowest risks of toxicity and the most significant potential for therapeutic application.

Table 2. Toxicity predictions.

Compound	Name	Predicted Toxicity Class	Predicted LD_{50}	Final Score
178	Ergosta-4,6,8(14),22-tetraen-3-one	6	10,000 mg/kg	309
18	5α,8α-Epidioxy-24(R)-methylcholesta-6,22-dien-3β-D-glucopyranoside	6	39,800 mg/kg	309
34	Polyporusterone A	6	9000 mg/kg	307
182	Lucidumol A	6	5010 mg/kg	306
26	Antcin K	6	9000 mg/kg	305
126	Inonotusol B	6	9000 mg/kg	303
3	3β,5α,8α,22E)-5,8-Epidioxyergosta-6,22-dien-3-ylβ-D-glucopyranoside	5	4000 mg/kg	264
4	(22*E*,24*S*)-Ergosta-4,22-dien-3-one	5	2300 mg/kg	263
130	Inonotusol F	5	5000 mg/kg	263
154	3,11-Dioxolanosta-8,24(*Z*)-diene-26-oic acid	5	3389 mg/kg	262
139	Inonotsuoxides A	5	3520 mg/kg	262
45	Aurisin A	5	2500 mg/kg	262
140	Inonotsuoxides B	5	3520 mg/kg	262
124	Acetyl-3-oxo-sulfurenic acid (64)	5	5000 mg/kg	261
17	5α,6α-Epoxy-24(*R*)-methylcholesta-7,22-dien-3β-ol	5	5000 mg/kg	261
181	Cerevisterol	5	2340 mg/kg	261
19	5α,8α-Epidioxy-24(*R*)-methylcholesta-6,22-dien-β-ol	5	5000 mg/kg	261
6	(22*E*)-6β-Methoxyergosta-7,22-diene-3β,5α-diol	5	2340 mg/kg	260
194	Ganoderic Acid T	5	3000 mg/kg	259
111	Officimalonic acids D	5	3267 mg/kg	258
191	Ganoderic Acid W	5	3000 mg/kg	258
192	Ganoderic Acid X	5	5000 mg/kg	258
113	Officimalonic acids F	5	3267 mg/kg	258
195	Polyporenic acid C	5	5000 mg/kg	257
121	Lanostanoid 4	4	1000 mg/kg	218
7	(22*E*)-19-Norergosta-5,7,9,22-tetraen-3β-ol	4	590 mg/kg	218
133	Inonotsudiol A	4	2000 mg/kg	218
134	Inonotsuoxodiol A	4	1000 mg/kg	218
23	Eburicoic acid	4	1000 mg/kg	217
193	Ganoderic Acid Y	4	1000 mg/kg	217
13	24-Ethylcholesta-5,22-dien-3β-ol	4	890 mg/kg	217
Control	Tariquidar	4	1570 mg/kg	217

Only the compounds with the best classification are shown in this table. Complete table available in Supplementary Materials.

3.3. ADME Analysis

Based on the analyses of the ADME parameters and the scoring system described above, it was possible to identify bioactive compounds with different pharmacokinetic profiles (Table 3). An ADME score was calculated based on the predicted pharmacokinetic properties of the compounds, and a scale from 1 to 4 was calculated as described before. Of the 31 compounds selected in the toxicity prediction analysis, six compounds presented the highest ADME scores (ADME score = 4): ergosta-4,6,8(14),22-tetraen-3-one, antcin K, 3,11-dioxolanosta-8,24(*Z*)-diene-26-oic acid, lucidumol A, (22*E*)-19-norergosta-5,7,9,22-tetraen-3β-ol, and (22*E*,24*S*)-ergosta-4,22-dien-3-one. In general, these six compounds presented good oral bioavailability, as suggested by their high predicted GI absorption values. In the analysis, only four compounds did not prove to be P-gp substrates, three of which were classified among the six most promising in this screening, as well as the positive control tariquidar. Among the six most promising compounds, three showed a violation of Lipinski's Rule. The compounds (22*E*,24*S*)-ergosta-4,22-dien-3-one and (22*E*)-19-norergosta-5,7,9,22-tetraen-3β-ol showed Moriguchi octanol–water partition coefficient (MLOGP) values $>$ 4.15, indicating high lipophilicity. In addition, the compound (22*E*)-19-norergosta-5,7,9,22-tetraen-3β-ol had a molecular weight (MW) > 500 g/mol, indicating a relatively high mass. Potential to cross the BBB was demonstrated by the compounds ergosta-4,6,8(14),22-tetraen-3-one, (22*E*,24*S*)-ergosta-4,22-dien-3-one, and (22*E*)-19-norergosta-5,7,9,22-tetraen-3β-ol. Polyporusterone A, inonothoxides A/B, acetyl-3-oxo-sulfurenic acid (64), cerevisterol, (22E)-6β-methoxy-ergosta-7,22-diene-3β,5α-diol, ganoderic acid X, officimalonic acids F, polyporenic acid C, and inonothoxodiol A were among the compounds with an ADME classification score of 3. Except for polyporusterone A, which showed minimal absorption, they all showed high GI absorption and were considered P-gp substrates. In the evaluation of Lipinski's Rule, there was one violation, generally related to MLOGP $>$ 4.15, and, in the case of officimalonic acids F, the molecular weight (MW) $>$ 500 daltons. Among the compounds analyzed through the virtual screening pipeline implemented, six compounds stood out as exhibiting superior P-gp predicted binding energies, favorable toxicological profiles, and promising ADME characteristics: ergosta-4,6,8(14),22-tetraen-3-one (Figure 5(1a,1b)), lucidumol A (Figure 5(2a,2b)), antcin K (Figure 5(3a,3b)), (22*E*,24*S*)-ergosta-4,22-dien-3-one (Figure 5(4a,4b)), 3,11-dioxolanosta-8,24(*Z*)-diene-26-oic acid (Figure 5(5a,5b)), and (22*E*)-19-norergosta-5,7,9,22-tetraen-3β-ol (Figure 5(6a,6b)). These six compounds consistently demonstrated high values across various favorable parameters, suggesting their viability for therapeutic applications. They are strong candidates for further investigation.

Table 3. ADME analysis results.

Compound	Name	P-gp Substrate	GI Absorption$_{50}$	BBB Permeant	Lipinski's Rule of Five	ADME Score
178	Ergosta-4,6,8(14),22-tetraen-3-one	No	High	Yes	Yes; 1 violation: MLOGP > 4.15	4
182	Lucidumol A	Yes	High	No	Yes; 0 violations	4

Table 3. *Cont.*

Compound	Name	P-gp Substrate	GI Absorption$_{50}$	BBB Permeant	Lipinski's Rule of Five	ADME Score
26	Antcin K	Yes	High	No	Yes; 0 violations	4
4	(22*E*,24*S*)-Ergosta-4,22-dien-3-one	No	High	Yes	Yes; 1 violation: MLOGP > 4.15	4
154	3,11-Dioxolanosta-8,24(*Z*)-diene-26-oic acid	Yes	High	No	Yes; 0 violations	4
7	(22*E*)-19-Norergosta-5,7,9,22-tetraen-3β-ol	No	High	Yes	Yes; 1 violation: MLOGP > 4.15	4
Control	Tariquidar	No	Low	No	Yes; 1 violation: MW > 500	4

Only the compounds with the best classification are shown in this table. Complete table available in Supplementary Materials.

4. Discussion

Cancer is one of the greatest causes of death worldwide, with estimates pointing to a significant increase in the number of new cases, which is expected to reach 35 million by 2050 [38]. Chemotherapy remains the primary therapeutic strategy in the fight against cancer, but multidrug resistance (MDR) compromises its effectiveness in around 90% of cases. The reason for this is that tumor cells develop resistance to antitumor compounds, leading to tumor cell invasion and metastasizing [39,40]. The overexpression of P-glycoprotein (P-gp) promotes the efflux of chemotherapeutic drugs from tumor cells, reducing their intracellular concentrations and efficacy. This MDR mechanism, which has already been identified in various types of cancer, impairs the efficacy of routinely used drugs such as doxorubicin, 5-fluorouracil, paclitaxel, and cisplatin [40,41]. Searching for natural compounds, such as those derived from mushrooms, is promising because they exhibit an MDR inhibition capacity while maintaining low toxicity, indicating potential to enhance the efficacy of cancer treatments. Molecular docking is a valuable tool for predicting interactions between bioactive substances and molecular targets, offering insights into their mechanisms of action. This method efficiently predicts ligand–receptor affinities by evaluating the binding energy. Lower binding energies indicate stronger and more stable interactions, which are crucial in identifying promising compounds [42–44]. This method was first validated by redocking tariquidar against P-gp (PDB: 7A6E), which produced an RMSD value of 1.60 ÅṪhis result confirms the docking predictions' accuracy and the methodology's robustness. RMSD values less than 2 Å are typically ideal in verifying the conformance and guaranteeing the reliability of the used model [45].

After validation, the first screening stage of this work was to apply the molecular docking technique to predict the P-gp inhibition of the 211 compounds present in the mushroom database [21–23]. The analysis results are summarized in Figure 6, which presents an integrated heat map showcasing the predicted binding energy, toxicity prediction, and ADME performance for the top-ranking tested compounds. The results showed a wide range of potential interactions with P-gp, with binding energies ranging from −13.19 to 0.07 kcal/mol. The compounds with the strongest among those analyzed were lanostanoid 4 (−13.19 kcal/mol), lanostanoid 3 (−12.673 kcal/mol), and

(22*E*,24*S*)-ergosta-4,22-dien-3-one (−12.31 kcal/mol). Notably, of the 211 compounds present in the database, 59 compounds showed lower binding energies compared to the positive control, tariquidar (−10.78 kcal/mol), a strong and well-known P-gp inhibitor [44], indicating greater potential for these compounds. Figure 6 presents the results of 31 compounds that presented lower predicted binding energies and better predicted toxicity profiles. The analysis of the molecular contact surface (Con.Surf[A^2]) provides information about the degree of physical interaction between the ligand and the receptor. Greater contact surface areas indicate more extensive interactions, which may favor the stability of the complex. Tariquidar exhibited the largest contact surface (633.75 A^2) and is defined as a molecule with a large molecular surface area. However, other compounds, such as officimalonic acids G (562.15 A^2), officimalonic acids D (565.94 A^2), and ganoderic acid T (587.44 A^2) also showed significative areas, demonstrating their strong interaction capacity. On the other hand, compounds such as ergosta-4,6,8(14),22-tetraen-3-one (367.21 A^2), (22*E*)-19-norergosta-5,7,9,22-tetraen-3β-ol (384.84 A^2), and eringiacetal A (388.48 A^2) showed lower values, indicating less extensive interactions. To choose the least harmful compounds, toxicity prediction was performed in the second step, considering the 59 compounds with the lowest binding energies in the previous phase. Of these 59 compounds, 31 were predicted to be less toxic when compared to the control. In our toxicity predictions, most compounds showed a low probability of causing liver damage. On the other hand, it was found that many may be potentially neurotoxic and toxic to the respiratory system. In a previous study, an ergosterol derivative, ergosta-7,9(11),22-trien-3β-ol, isolated from the mycelium of *Antrodia camphorate*, was administered to male rats in three groups for six weeks to assess its effects on ergogenic function and fatigue. According to the data, supplementation with ergosta-7,9(11),22-trien-3β-ol did not cause histological changes in the primary organs evaluated (i.e., liver, muscle, heart, kidney, lung, and epididymal fat pad) [46]. These results corroborate our findings, since compounds such as ergosterol and (22*E*)-ergosta-5,7,22-trien-3β-ol did not show hepatotoxicity, cardiotoxicity, or nephrotoxicity. On the other hand, the results are contradictory with regard to respiratory toxicity. With regard to nephrotoxicity, some compounds stood out as having high predicted toxicity, associated with low LD_{50} values. However, several other compounds also showed significant toxicity. The most concerning compounds are colossolactone H (LD_{50} = 9 mg/kg) and officimalonic acids C (LD_{50} = 10 mg/kg), followed by officimalonic acids G (LD_{50} = 79 mg/kg) and ganoderic acid H (LD_{50} = 200 mg/kg). However, one study showed that a triterpenoid, ganoderic acid A, has the ability to relieve kidney inflammation in mice, improving kidney function by regulating antioxidant activity (Trx/TrxR, GSH, SOD, GPx) and inhibiting the JAK2/STAT3, RhoA/ROCK, NF-kB, and TGF-β/Smad3 pathways [47]. In another study, ganoderic acid was able to protect against renal lesions caused by ischemia–reperfusion, reducing inflammation by inhibiting TLR4/MyD88/NF-kB and reducing apoptosis, as evidenced by the reduction of caspases-3 and -8 and inhibition of apoptosis in the mice [48]. Regarding colossolactone H, no studies were found evaluating the nephrotoxicity of this compound. However, a study showed that this triterpenoid isolated from *Ganoderma colossum* exhibited high cytotoxicity, interfering with the cell cycle, causing apoptosis, and increasing ROS, thus resulting in DNA damage and the activation of the p53 protein, as well as exhibiting synergistic action with gefitinib, reducing tumors in resistant cells and in mouse models [49]. Most of the compounds analyzed were classified as active, which suggests a considerable impact on the respiratory system. All compounds except ergosta-4,6,8(14),22-tetraen-3-one showed inactive toxicity. This general trend indicates potential respiratory risks that require further research within a safety analysis. The compounds vary in their toxicity endpoints. With regard to carcinogenicity, 35 compounds showed toxic activity and 25 showed no

toxicity. With regard to toxicity to the immune system, most compounds showed active toxicity, while only 10 compounds demonstrated inactive toxicity. On the other hand, mutagenic activity was non-existent for most of the compounds, with the exception of piptolinic acid E, which showed active cytotoxicity. Regarding the BBB barrier, most of the compounds showed potential toxicity, but only four showed inactive toxicity. Many compounds were innocuous in terms of ecotoxicity, but 15 may have some effect on the environment. Regarding clinical and nutritional toxicity, most of them pose some danger to human health. The results of the evaluation of toxicity in the nuclear receptor signaling pathways showed that all compounds analyzed did not show toxicity towards receptors such as AhR, ER-LBD, aromatase, and PPAR-Gamma, indicating reduced potential for interference in the endocrine and metabolic systems. With regard to the ER receptor, only officimalonic C and ganoderic T acids showed toxic activity. As for the AR and AR-LBD receptors, there was a more marked variation in the results, suggesting variations in the interactions of the compounds with these targets. The results showed that most of the compounds analyzed regarding the stress response pathways exhibited inactive toxicity in the markers evaluated, indicating low potential to cause stress in cells. Notably, no compounds exhibited active toxicity in the p53 and ATAD5 markers, which is significant as it suggests a lack of interference in critical pathways for tumor suppression and the maintenance of DNA integrity, which are essential factors in preventing carcinogenesis. The tumor suppressor p53 is often called the 'guardian of the genome' because of its crucial role in preserving genomic stability [50]. ATAD5 also plays a vital in preserving genomic stability [51]. The toxic inactivity profile indicates a rescued risk of causing or promoting cancer, corroborating the genomic safety of the compounds. In the prediction of toxicity in molecular initiating events, all compounds showed inactive toxicity regarding the THRβ, RYR, NMDAR, AMPAR, KAR, CAR, VGSC, and NIS receptors. However, regarding the THRα receptor, the compounds ganoderic acid W, H, X, and F, aurisin A, inoscavin A, lanostanoid 3, and officimalonic acids F, E, and G showed active toxicity. In the TTR, only aurisin A, inoscavin A, and lanostanoid 3 showed active toxicity. For the GABA receptor, most of the compounds showed inactive toxicity, but 47 of the compounds were active. With regard to AChE, only the compounds tariquidar and colossolactone H showed active toxicity. In NADHOX, the compounds (3β,5α,8α,22E)-5,8-epidioxyergosta-6,22-dien-3-yl β-D-glucopyranoside, eringiacetal A, officimalonic acids C, and colossolactone H showed active toxicity. For the PXR receptor, there was greater variability. In the toxicity assessment in terms of metabolism, all compounds were considered non-toxic to the cytochromes CYP1A2, CYP2C19, CYP2D6, and CYP2E1—enzymes that perform essential functions in the metabolism of medicines and substances [37]. However, 12 compounds showed toxicity to cytochrome CYP2C9. The control tariquidar and compound inonotusol F showed toxicity to cytochrome CYP3A4. Finally, the pharmacokinetic characteristics were evaluated to identify promising modulators of P-gp activity. Based on the analyses of the ADME parameters and the scoring system developed, it was possible to identify that six compounds showed better pharmacokinetic potential than our control. The compounds with the highest scores (ADME = 4) and selected as the most promising from this screening were ergosta-4,6,8(14),22-tetraen-3-one, lucidumol A, antcin K, (22*E*,24*S*)-ergosta-4,22-dien-3-one, 3,11-dioxolanosta-8,24(*Z*)-diene-26-oic acid, and (22*E*)-19-norergosta-5,7,9,22-tetraen-3β-ol, which obtained the same scores as the control, tariquidar. These compounds stood out for their excellent oral bioavailability, proven by their predicted high absorption in the GI system. Furthermore, as they are not P-gp substrates, their efficacy in therapies against resistance mediated by this protein is likely to be increased. Only the sterol derivatives (ergosta-4,6,8(14),22-tetraen-3-one; (22*E*,24*S*)-ergosta-4,22-dien-3-one, and (22*E*)-19-norergosta-5,7,9,22-tetraen-3β-ol) could cross the BBB. Some P-gp modulators

are competitive inhibitors of the ability of anticancer drugs to bind to P-gp. However, they are also P-gp substrates and are expelled from cells [52]. Only the compounds (22*E*,24*S*)-ergosta-4,22-dien-3-one and (22*E*)-19-norergosta-5,7,9,22-tetraen-3β-ol violated Lipinski's Rule of Five—specifically, the criterion MLOGP > 4.15—indicating high lipophilicity. Additionally, the control compound tariquidar violated the rule regarding the molecular weight (MW > 500 Da). Although they pose a challenge, these violations are common in natural products, which often have high biological potential. Optimization strategies can overcome these limitations. Tariquidar is an example of this; despite its violations and toxicity, it has progressed to clinical trials. Therefore, such cases should be evaluated flexibly in the early stages of development. This research's findings align with previous studies that have shown that cancer cells with microRNA-378 are more aggressive and resistant to drugs, requiring higher doses of chemotherapy to be eradicated. However, therapy with ergosterol peroxide, obtained from *Ganoderma lucidum*, overcomes this resistance, inducing the cell's death more efficiently, even at lower doses [53]. In a more recent study, an ethanolic extract of *Ganoderma lucidum* showed an ability to reverse MDR in cells and mice with resistant hepatocellular carcinoma, inhibiting the activity of P-gp without modifying its expression levels [54]. Although no studies have been found on the modulation of P-gp by the compound ergosta-4,6,8(14),22-tetraen-3-one, some studies have highlighted the antitumor potential of this compound and its derivatives. One study demonstrated antiproliferative activity in hepatocellular carcinoma cells (HepG2), induced by caspase-mediated apoptosis, with the interruption of the cell cycle in G2/M and changes in the regulation of Bax and Bcl-2 [55]. In another study, the same compound extracted from *Antrodia cinnamomea* reduced cancer-initiating cells in head and neck carcinoma, inhibiting STAT3 and Src, promoting cell differentiation, and restoring chemosensitivity in combination with chemotherapy [56]. We found no specific studies evaluating lucidumol A in the modulation of P-gp. However, research has shown that lucidumol D, extracted from *Ganoderma lingzhi*, exhibits selective cytotoxicity towards the MCF-7, HepG2, HeLa, Caco-2, and HCT-116 cancer cell lines [57]. Additionally, in another study, lucidumol A extracted from *Ganoderma lucidum* was shown to have an effective anticancer and anti-inflammatory effects against colorectal cancer and RAW264.7 cells. In in vitro studies, this compound reduced the metastatic potential at low concentrations and reduced inflammatory markers and cytokine levels in RAW264.7 cells subjected to treatment [20]. It is important to note that these cell lines were not described by the authors as cells with the overexpression of P-gp. The results of this study and previous research show that certain compounds from mushrooms may overcome MDR. These compounds are predicted to have a high affinity for P-gp, exhibit low toxicity, and have interesting pharmacokinetic properties, suggesting that they may render cancer cells more sensitive to chemotherapy treatments, according to molecular docking studies. These findings imply that these substances could be used as possible aids in cancer therapy, increasing the effectiveness of medication and decreasing the resistance to traditional treatments. This in silico work provides a predictive model, but more research is needed to elucidate and validate the therapeutic safety of these drugs.

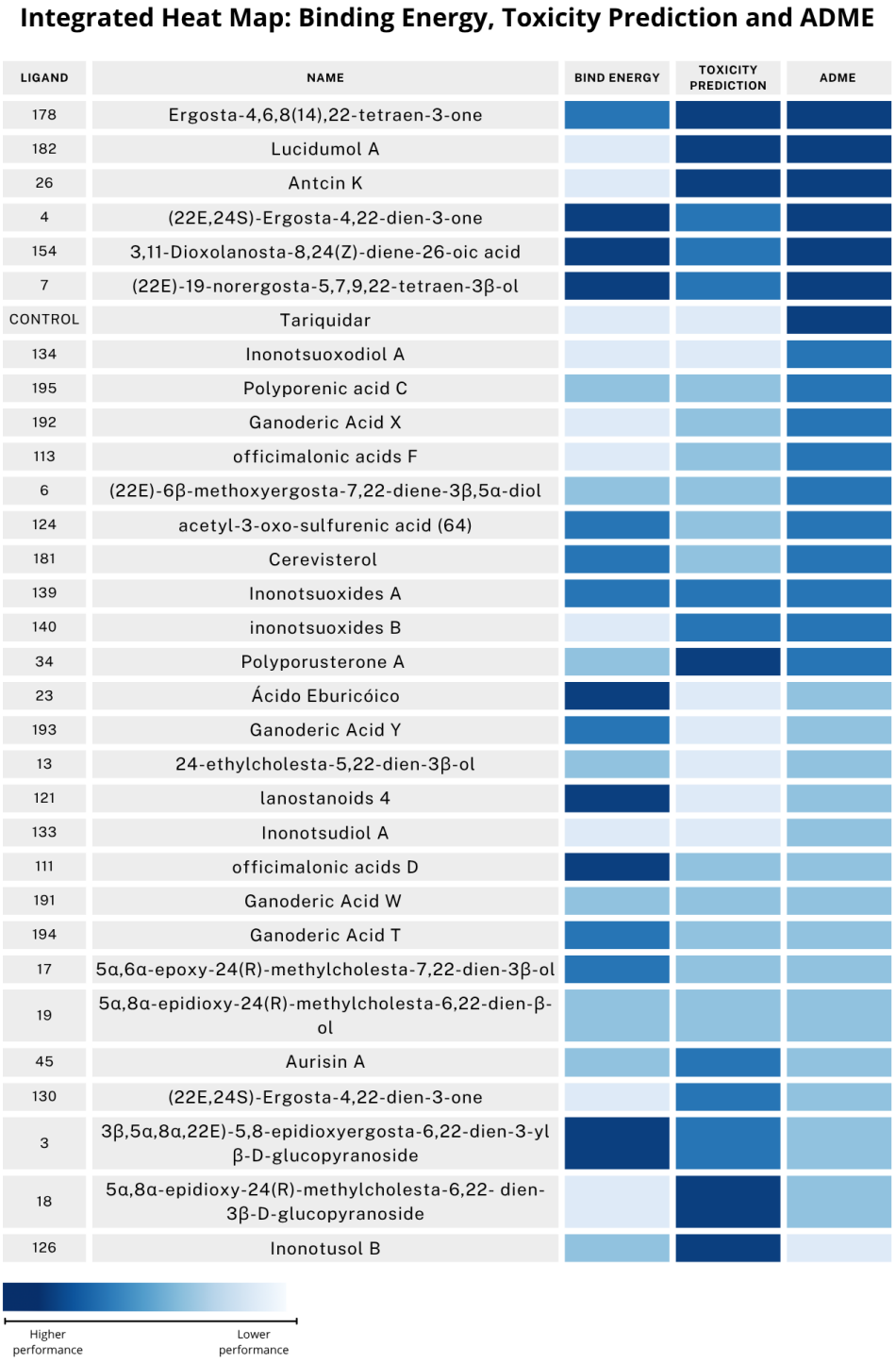

Figure 6. Integrated heat map showing the results regarding the binding energies, toxicity predictions, and ADME properties of mushroom compounds studied for interactions with the P-gp protein. Each row represents a compound identified by its name and code, while the columns indicate their performance in each parameter evaluated. The coloring varies from darker shades, which represent better performance (lower binding energy and greater safety/reduced toxicity), to lighter shades, which indicate lower efficiency. The compounds are ranked in order of overall performance, with an emphasis on those with the greatest potential for interacting with P-gp. The positive control (tariquidar) is included for comparison.

5. Conclusions

Based on the results obtained, this study identified six mushroom compounds as potential modulators of P-glycoprotein (P-gp), an important target in overcoming multidrug resistance (MDR) in tumor cells. The compounds ergosta-4,6,8(14),22-tetraen-3-one, lucidumol A, antcin K, (22*E*,24*S*)-ergosta-4,22-dien-3-one, 3,11-dioxolanosta-8,24(*Z*)-diene-26-oic acid, and (22*E*)-19-norergosta-5,7,9,22-tetraen-3β-ol showed the best binding affinities, low predicted toxicity, and favorable pharmacokinetic properties. These findings provide a solid basis for further experimental investigations to contribute to advancements in the efficacy of oncological treatments.

Supplementary Materials: The following supporting information can be downloaded at: https://www.mdpi.com/article/10.3390/app15168772/s1. Table S1: Redoocking Results. Table S2: Best poses redocking. Table S3: Virtual screening with molecular docking. Table S4: Toxicity Prediction. Table S5: ADME analysis.

Author Contributions: J.F.—conceptualization, methodology, data curation, writing—original draft, molecular docking techniques, computational analyses and editing, visualization and illustrations; C.S.H.S.—molecular docking techniques, computational analyses, writing—review and editing; R.M.V.A.—critical revision of the manuscript, data interpretation, overall refinement of the study; S.R.—critical revision of the manuscript, data interpretation, overall refinement of the study; J.A.V.—critical revision of the manuscript, data interpretation, overall refinement of the study. All authors have read and agreed to the published version of the manuscript.

Funding: The authors would like to thank CESPU—Cooperativa de Ensino Superior Politécnico e Universitário—for the PhD scholarship BD/DCB/CESPU/01/2023 awarded to Jéssica Fonseca and the Fundação para a Ciência e Tecnologia (FCT), Portugal, for the PhD scholarship 2023.04950.BD awarded to Carlos S.H. Shiraish. This work was funded by national funds from the FCT—Fundação para a Ciência e a Tecnologia, I.P.—under the project/support number UID/6157/2023.

Data Availability Statement: The original contributions presented in this study are included in the article/supplementary material. Further inquiries can be directed to the corresponding authors.

Conflicts of Interest: The authors declare no conflicts of interest.

References

1. Goebel, J.; Chmielewski, J.; Hrycyna, C.A. The roles of the human ATP-binding cassette transporters P-glycoprotein and ABCG2 in multidrug resistance in cancer and at endogenous sites: Future opportunities for structure-based drug design of inhibitors. *Cancer Drug Resist.* **2021**, *4*, 784. [CrossRef]
2. Park, H.J. Current uses of mushrooms in cancer treatment and their anticancer mechanisms. *Int. J. Mol. Sci.* **2022**, *23*, 10502. [CrossRef]
3. Mora Lagares, L.; Pérez-Castillo, Y.; Minovski, N.; Novič, M. Structure–function relationships in the human P-glycoprotein (ABCB1): Insights from molecular dynamics simulations. *Int. J. Mol. Sci.* **2021**, *23*, 362. [CrossRef]
4. Nanayakkara, A.K.; Follit, C.A.; Chen, G.; Williams, N.S.; Vogel, P.D.; Wise, J.G. Targeted inhibitors of P-glycoprotein increase chemotherapeutic-induced mortality of multidrug resistant tumor cells. *Sci. Rep.* **2018**, *8*, 967. [CrossRef] [PubMed]
5. Waghray, D.; Zhang, Q. Inhibit or evade multidrug resistance P-glycoprotein in cancer treatment: Miniperspective. *J. Med. Chem.* **2017**, *61*, 5108–5121. [CrossRef] [PubMed]
6. Mahmud, S.; Islam, M.J.; Parves, M.R.; Khan, M.A.; Tabussum, L.; Ahmed, S.; Ali, M.A.; Fakayode, S.O.; Halim, M.A. Designing potent inhibitors against the multidrug resistance P-glycoprotein. *J. Biomol. Struct. Dyn.* **2022**, *40*, 9403–9415. [CrossRef] [PubMed]
7. Marques, S.M.; Šupolíková, L.; Molčanová, L.; Šmejkal, K.; Bednar, D.; Slaninová, I. Screening of natural compounds as P-glycoprotein inhibitors against multidrug resistance. *Biomedicines* **2021**, *9*, 357. [CrossRef]
8. Yang, Z.; Cai, Y.; Yang, X.; Li, Y.; Wu, Q.; Yu, Y.; Chen, Z.; Wei, B.; Tian, J.M.; Bao, X.; et al. Novel benzo five-membered heterocycle derivatives as P-glycoprotein inhibitors: Design, synthesis, molecular docking, and anti-multidrug resistance activity. *J. Med. Chem.* **2023**, *66*, 5550–5566. [CrossRef]

9. Afonso de Lima, C.; de Souza Bueno, I.L.; Nunes Siqueira Vasconcelos, S.; Sciani, J.M.; Ruiz, A.L.T.G.; Foglio, M.A.; Carvalho, J.E.d.; Barbarini Longato, G. Reversal of ovarian cancer cell lines multidrug resistance phenotype by the association of apiole with chemotherapies. *Pharmaceuticals* **2020**, *13*, 327. [CrossRef]
10. Calhelha, R.C.; Shiraishi, C.S.; Ribeiro, L.; Carocho, M.; Abreu, R.; Coutinho, P.; Barros, L.; Vaz, J.; Ferreira, I.C. New Trends from Fungi Secondary Metabolism in the Pharmaceutical Industry. In *Natural Secondary Metabolites: From Nature, Through Science, to Industry*; Springer: Berlin/Heidelberg, Germany, 2023; pp. 823–850.
11. Wang, L.; Sun, Y. Efflux mechanism and pathway of verapamil pumping by human P-glycoprotein. *Arch. Biochem. Biophys.* **2020**, *696*, 108675. [CrossRef]
12. Dewanjee, S.; Dua, T.K.; Bhattacharjee, N.; Das, A.; Gangopadhyay, M.; Khanra, R.; Joardar, S.; Riaz, M.; De Feo, V.; Zia-Ul-Haq, M. Natural products as alternative choices for P-glycoprotein (P-gp) inhibition. *Molecules* **2017**, *22*, 871. [CrossRef]
13. Nagy, H.; Goda, K.; Fenyvesi, F.; Bacsó, Z.; Szilasi, M.; Kappelmayer, J.; Lustyik, G.; Cianfriglia, M.; Szabó Jr, G. Distinct groups of multidrug resistance modulating agents are distinguished by competition of P-glycoprotein-specific antibodies. *Biochem. Biophys. Res. Commun.* **2004**, *315*, 942–949. [CrossRef]
14. Mollazadeh, S.; Sahebkar, A.; Hadizadeh, F.; Behravan, J.; Arabzadeh, S. Structural and functional aspects of P-glycoprotein and its inhibitors. *Life Sci.* **2018**, *214*, 118–123. [CrossRef]
15. Gou, Y.; Zheng, X.; Li, W.; Deng, H.; Qin, S. Polysaccharides produced by the mushroom trametes robiniophila murr boosts the sensitivity of hepatoma cells to oxaliplatin via the miR-224-5p/ABCB1/P-gp Axis. *Integr. Cancer Ther.* **2022**, *21*, 15347354221090221. [CrossRef] [PubMed]
16. Doğan, H.H.; Kars, M.D.; Özdemir, Ö.; Gündüz, U. Fomes fomentarius and Tricholoma anatolicum (Agaricomycetes) extracts exhibit significant multiple drug-resistant modulation activity in drug-resistant breast cancer cells. *Int. J. Med. Mushrooms* **2020**, *22*, 105–114. [CrossRef] [PubMed]
17. Xu, W.W.; Li, B.; Lai, E.T.C.; Chen, L.; Huang, J.J.H.; Cheung, A.L.M.; Cheung, P.C.K. Water extract from Pleurotus pulmonarius with antioxidant activity exerts in vivo chemoprophylaxis and chemosensitization for liver cancer. *Nutr. Cancer* **2014**, *66*, 989–998. [CrossRef]
18. Teng, Y.N.; Chang, C.S.; Lee, T.E.; Hung, C.C. Cordycepin re-sensitizes multidrug resistance cancer cells to chemotherapeutic agents through modulating P-glycoprotein expression and ATPase function. *J. Funct. Foods* **2016**, *26*, 681–690. [CrossRef]
19. Fonseca, J.; Vaz, J.A.; Ricardo, S. The potential of mushroom extracts to improve chemotherapy efficacy in cancer cells: A systematic review. *Cells* **2024**, *13*, 510. [CrossRef]
20. Shin, M.J.; Chae, H.J.; Lee, J.W.; Koo, M.H.; Kim, H.J.; Seo, J.B.; YanIllia, S.; Park, S.H.; Lo, H.E.; Kim, S.H.; et al. Lucidumol A, Purified Directly from Ganoderma lucidum, Exhibits Anticancer Effect and Cellular Inflammatory Response in Colorectal Cancer. *Evid.-Based Complement. Altern. Med.* **2022**, *2022*, 7404493. [CrossRef]
21. CFR Ferreira, I.; Vaz, J.A.; Vasconcelos, M.H.; Martins, A. Compounds from wild mushrooms with antitumor potential. *Anti-Cancer Agents Med. Chem.-Anti Agents* **2010**, *10*, 424–436. [CrossRef]
22. Borges, B.F. Preparação e Screening Virtual de uma Biblioteca de Compostos de Baixo Peso Molecular Oriundos de Cogumelos Contra Proteínas da Família BCL-2. Master's Thesis, Instituto Politecnico de Braganca (Portugal), Bragança, Portugal, 2018.
23. Shiraishi, C.S.H. Estudo do Potencial Anti-inflamatório de Uma Biblioteca de Compostos Naturais de Cogumelos por Screening Virtual Contra as Enzimas Cox (-1 E-2). Master's Thesis, Instituto Politecnico de Braganca (Portugal), Bragança, Portugal, 2020.
24. Li, W.; Zhang, H.; Assaraf, Y.G.; Zhao, K.; Xu, X.; Xie, J.; Yang, D.H.; Chen, Z.S. Overcoming ABC transporter-mediated multidrug resistance: Molecular mechanisms and novel therapeutic drug strategies. *Drug Resist. Updat.* **2016**, *27*, 14–29. [CrossRef] [PubMed]
25. Thomas, H.; Coley, H.M. Overcoming multidrug resistance in cancer: An update on the clinical strategy of inhibiting p-glycoprotein. *Cancer Control* **2003**, *10*, 159–165. [CrossRef]
26. Gagliano, T.; Gentilin, E.; Benfini, K.; Di Pasquale, C.; Tassinari, M.; Falletta, S.; Feo, C.; Tagliati, F.; Uberti, E.d.; Zatelli, M.C. Mitotane enhances doxorubicin cytotoxic activity by inhibiting P-gp in human adrenocortical carcinoma cells. *Endocrine* **2014**, *47*, 943–951. [CrossRef]
27. Consoli, U.; Priebe, W.; Ling, Y.H.; Mahadevia, R.; Griffin, M.; Zhao, S.; Perez-Soler, R.; Andreeff, M. The novel anthracycline annamycin is not affected by P-glycoprotein-related multidrug resistance: Comparison with idarubicin and doxorubicin in HL-60 leukemia cell lines. *Blood* **1996**, *88*, 633–644. [CrossRef]
28. Sander, T.; Freyss, J.; Von Korff, M.; Rufener, C. DataWarrior: An open-source program for chemistry aware data visualization and analysis. *J. Chem. Inf. Model.* **2015**, *55*, 460–473. [CrossRef]
29. Land, H.; Humble, M.S. YASARA: A tool to obtain structural guidance in biocatalytic investigations. In *Protein Engineering: Methods and Protocols*; Humana Press: New York, NY, USA, 2018; pp. 43–67.
30. Nosol, K.; Romane, K.; Irobalieva, R.N.; Alam, A.; Kowal, J.; Fujita, N.; Locher, K.P. Cryo-EM structures reveal distinct mechanisms of inhibition of the human multidrug transporter ABCB1. *Proc. Natl. Acad. Sci. USA* **2020**, *117*, 26245–26253. [CrossRef]

31. Trott, O.; Olson, A. Software news and update AutoDock Vina: Improving the speed and accuracy of docking with a new scoring function. *Effic. Optim. Multithreading* **2009**, *31*, 455–461.
32. Bell, E.W.; Zhang, Y. DockRMSD: An open-source tool for atom mapping and RMSD calculation of symmetric molecules through graph isomorphism. *J. Cheminform.* **2019**, *11*, 40. [CrossRef]
33. Schrödinger, LLC. *The PyMOL Molecular Graphics System, Version 1.8*; Schrödinger, LLC: New York, NY, USA, 2015.
34. Schöning-Stierand, K.; Diedrich, K.; Ehrt, C.; Flachsenberg, F.; Graef, J.; Sieg, J.; Penner, P.; Poppinga, M.; Ungethüm, A.; Rarey, M. Proteins Plus: A comprehensive collection of web-based molecular modeling tools. *Nucleic Acids Res.* **2022**, *50*, W611–W615. [CrossRef] [PubMed]
35. Banerjee, P.; Kemmler, E.; Dunkel, M.; Preissner, R. ProTox 3.0: A webserver for the prediction of toxicity of chemicals. *Nucleic Acids Res.* **2024**, *52*, W513–W520. [CrossRef]
36. Daina, A.; Michielin, O.; Zoete, V. SwissADME: A free web tool to evaluate pharmacokinetics, drug-likeness and medicinal chemistry friendliness of small molecules. *Sci. Rep.* **2017**, *7*, 42717. [CrossRef] [PubMed]
37. Zhao, M.; Ma, J.; Li, M.; Zhang, Y.; Jiang, B.; Zhao, X.; Huai, C.; Shen, L.; Zhang, N.; He, L.; et al. Cytochrome P450 enzymes and drug metabolism in humans. *Int. J. Mol. Sci.* **2021**, *22*, 12808. [CrossRef] [PubMed]
38. Bray, F.; Laversanne, M.; Sung, H.; Ferlay, J.; Siegel, R.L.; Soerjomataram, I.; Jemal, A. Global cancer statistics 2022: GLOBOCAN estimates of incidence and mortality worldwide for 36 cancers in 185 countries. *CA Cancer J. Clin.* **2024**, *74*, 229–263. [CrossRef]
39. Toledo, B.; González-Titos, A.; Hernández-Camarero, P.; Perán, M. A brief review on chemoresistance; targeting cancer stem cells as an alternative approach. *Int. J. Mol. Sci.* **2023**, *24*, 4487. [CrossRef] [PubMed]
40. Tian, Y.; Lei, Y.; Wang, Y.; Lai, J.; Wang, J.; Xia, F. Mechanism of multidrug resistance to chemotherapy mediated by P-glycoprotein. *Int. J. Oncol.* **2023**, *63*, 119. [CrossRef]
41. Emran, T.B.; Shahriar, A.; Mahmud, A.R.; Rahman, T.; Abir, M.H.; Siddiquee, M.F.R.; Ahmed, H.; Rahman, N.; Nainu, F.; Wahyudin, E.; et al. Multidrug resistance in cancer: Understanding molecular mechanisms, immunoprevention and therapeutic approaches. *Front. Oncol.* **2022**, *12*, 891652. [CrossRef]
42. Pinzi, L.; Rastelli, G. Molecular docking: Shifting paradigms in drug discovery. *Int. J. Mol. Sci.* **2019**, *20*, 4331. [CrossRef]
43. Agu, P.; Afiukwa, C.; Orji, O.; Ezeh, E.; Ofoke, I.; Ogbu, C.; Ugwuja, E.; Aja, P. Molecular docking as a tool for the discovery of molecular targets of nutraceuticals in diseases management. *Sci. Rep.* **2023**, *13*, 13398. [CrossRef]
44. Wahono, C.S.; Syaban, M.F.R.; Pratama, M.Z.; Rahman, P.A.; Erwan, N.E. Exploring the potential of phytoconstituents from Phaseolus vulgaris L against CXC motif chemokine receptor 4 (CXCR4): A bioinformatic and molecular dynamic simulations approach. *Egypt. J. Med. Hum. Genet.* **2024**, *25*, 52. [CrossRef]
45. Castro-Alvarez, A.; Costa, A.M.; Vilarrasa, J. The performance of several docking programs at reproducing protein–macrolide-like crystal structures. *Molecules* **2017**, *22*, 136. [CrossRef]
46. Chen, Y.M.; Sung, H.C.; Kuo, Y.H.; Hsu, Y.J.; Huang, C.C.; Liang, H.L. The Effects of Ergosta-7, 9 (11), 22-trien-3β-ol from Antrodia camphorata on the Biochemical Profile and Exercise Performance of Mice. *Molecules* **2019**, *24*, 1225. [CrossRef]
47. Ma, J.Q.; Zhang, Y.J.; Tian, Z.K. Anti-oxidant, anti-inflammatory and anti-fibrosis effects of ganoderic acid A on carbon tetrachloride induced nephrotoxicity by regulating the Trx/TrxR and JAK/ROCK pathway. *Chem.-Biol. Interact.* **2021**, *344*, 109529. [CrossRef] [PubMed]
48. Shao, G.; He, J.; Meng, J.; Ma, A.; Geng, X.; Zhang, S.; Qiu, Z.; Lin, D.; Li, M.; Zhou, H.; et al. Ganoderic acids prevent renal ischemia reperfusion injury by inhibiting inflammation and apoptosis. *Int. J. Mol. Sci.* **2021**, *22*, 10229. [CrossRef]
49. Chen, S.Y.; Chang, C.L.; Chen, T.H.; Chang, Y.W.; Lin, S.B. Colossolactone H, a new Ganoderma triterpenoid exhibits cytotoxicity and potentiates drug efficacy of gefitinib in lung cancer. *Fitoterapia* **2016**, *114*, 81–91. [CrossRef] [PubMed]
50. Marei, H.E.; Althani, A.; Afifi, N.; Hasan, A.; Caceci, T.; Pozzoli, G.; Morrione, A.; Giordano, A.; Cenciarelli, C. p53 signaling in cancer progression and therapy. *Cancer Cell Int.* **2021**, *21*, 703. [CrossRef] [PubMed]
51. Park, S.H.; Kang, N.; Song, E.; Wie, M.; Lee, E.A.; Hwang, S.; Lee, D.; Ra, J.S.; Park, I.B.; Park, J.; et al. ATAD5 promotes replication restart by regulating RAD51 and PCNA in response to replication stress. *Nat. Commun.* **2019**, *10*, 5718. [CrossRef]
52. Wong, I.L.; Wang, B.C.; Yuan, J.; Duan, L.X.; Liu, Z.; Liu, T.; Li, X.M.; Hu, X.; Zhang, X.Y.; Jiang, T.; et al. Potent and nontoxic chemosensitizer of P-glycoprotein-mediated multidrug resistance in cancer: Synthesis and evaluation of methylated epigallocatechin, gallocatechin, and dihydromyricetin derivatives. *J. Med. Chem.* **2015**, *58*, 4529–4549. [CrossRef]
53. Wu, Q.P.; Xie, Y.Z.; Deng, Z.; Li, X.M.; Yang, W.; Jiao, C.W.; Fang, L.; Li, S.Z.; Pan, H.H.; Yee, A.J.; et al. Ergosterol peroxide isolated from Ganoderma lucidum abolishes microRNA miR-378-mediated tumor cells on chemoresistance. *PLoS ONE* **2012**, *7*, e44579. [CrossRef]
54. Li, J.; Cao, L.; Yuan, C.; Jiang, Z.; Cai, H.; Xu, W.; Han, Y.; Chen, L.; Zhang, Q.; Jiang, R.; et al. Ganoderma lucidum extract reverses hepatocellular carcinoma multidrug resistance via inhibiting the function of P-glycoprotein in vitro and in vivo. *Ital. J. Food Sci.* **2023**, *35*, 90–98. [CrossRef]

55. Zhao, Y.Y.; Shen, X.; Chao, X.; Ho, C.C.; Cheng, X.L.; Zhang, Y.; Lin, R.C.; Du, K.J.; Luo, W.J.; Chen, J.Y.; et al. Ergosta-4, 6, 8 (14), 22-tetraen-3-one induces G2/M cell cycle arrest and apoptosis in human hepatocellular carcinoma HepG2 cells. *Biochim. Biophys. Acta (BBA)-Gen. Subj.* **2011**, *1810*, 384–390. [CrossRef]
56. Chang, C.W.; Chen, Y.S.; Chen, C.C.; Chan, I.O.; Chen, C.C.; Sheu, S.J.; Lin, T.w.; Chou, S.H.; Liu, C.J.; Lee, T.C.; et al. Targeting cancer initiating cells by promoting cell differentiation and restoring chemosensitivity via dual inactivation of STAT3 and src activity using an active component of antrodia cinnamomea mycelia. *Oncotarget* **2016**, *7*, 73016. [CrossRef] [PubMed]
57. Amen, Y.M.; Zhu, Q.; Tran, H.B.; Afifi, M.S.; Halim, A.F.; Ashour, A.; Mira, A.; Shimizu, K. Lucidumol C, a new cytotoxic lanostanoid triterpene from Ganoderma lingzhi against human cancer cells. *J. Nat. Med.* **2016**, *70*, 661–666. [CrossRef] [PubMed]